The SUSIM Mg II Core-to-Wing Ratio Index

Linton Floyd[1], John Cook[2], and Lynn Herring[1]

[1]Interferometrics, 14120 Parke Long Court, Suite 103, Chantilly, VA 20151, USA

[2]Code 7668, E.O. Hulburt Center for Space Research, Naval Research Laboratory, Washington, DC 20375 USA

Abstract

The Solar Ultraviolet Spectral Irradiance Monitor (SUSIM) aboard the Upper Atmosphere Research Satellite (UARS) has been measuring the solar UV irradiance since October 1991, extending from the near maximum of solar cycle 22 to the declining phase of solar cycle 23. Among its daily scientific products is the Mg II core-to-wing ratio, a solar activity index based on spectral irradiance measurements of the strong Mg II absorption feature near 280 nm. The dimensionless Mg II index is ratio of the core irradiance to that of the quasi-continuum in the nearby wings, but whose precise definition varies from one experiment to another. Accordingly, it is relatively insensitive to instrumental changes since these tend to be common to both irradiances. Despite differences in instruments and algorithms, a high level of correlation among individual Mg II indices has been found. These properties have led Viereck et al. (2004) and others to construct a Mg II composite index, extending from 1978 to the present. Produced only a few days after measurements are taken, the SUSIM Mg II index (version V21r2), at 13+ years, is currently the longest instrumental Mg II time series available. We present aspects of the SUSIM Mg II algorithm and we compare the it with various solar spectral irradiances, other versions of the Mg II index, and with the $F_{10.7}$ index commonly used in modeling studies.

Background and Overview

The solar UV spectral irradiance, the spectral sum of radiant flux over the solar disk, plays the major role in determining the structure of the terrestrial atmosphere. Although it varies over a wide span of time scales, its dominant periodicities are of the solar rotation (∼13.5 day) and the solar activity cycle (∼27 day). Because all of the solar UV irradiance below 290 nm is absorbed in the atmosphere, measurements of it must be made from space. Further, the intense UV radation exposure causes the measuring instruments to degrade. This responsivity degradation must be tracked and accounted for in the UV data products. Among the methods employed are intercomparisons with stars, lamps, and with other better calibrated experiments. Accordingly, accurate solar UV irradiance measurements have proven to be difficult and costly.

To improve our knowledge of the solar UV irradiance and its variation, several models of it have been developed. Inevitably, these models must depend on solar measurements of various kinds, as an entirely deductive model of the solar irradiance does not and cannot exist. Most popular among these are the so-called proxy models which utilize daily solar measurements, often made from the ground, to characterize the level of solar activity. Irradiance measurements have been shown to vary with the level of solar activity. Measured daily since 1947, the solar 10.7 cm radio flux, better known as the $F_{10.7}$ index, has served as the basis of several proxy models of solar irradiance. Proxy models requiring earlier projections have instead the International Sunspot Number (ISN).

More recently, additional solar activity proxies such as the Equivalent Width of the He I 1083 cm line (He 1083) and the Mg II core-to-wing ratio (Mg II) have been constructed (Heath & Schlesinger, 1986). Their time series extend back to 1974 and 1978, respectively. Studies have shown these correlate with UV irradiance time series better than do $F_{10.7}$ and ISN (Donnelly et al., 1986; Floyd et al., 2004). The Mg II index is calculated for the strong Mg II absorption feature near 280 nm. Unlike the others, calculations of Mg II must be based on UV irradiance measurements from satellites. Mg II has been calculated from several UV irradiance experiments, including SUSIM. Here, we present the SUSIM Mg II core-to-wing ratio index, some aspects of its relationship with other Mg II indices, solar UV and EUV irradiances, and with the ISN, $F_{10.7}$, and He 1083 solar activity indices.

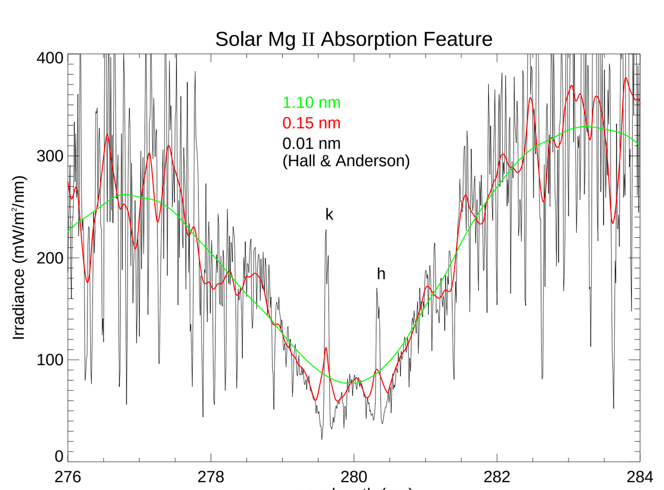

The SUSIM Mg II Index

In this section, we present the chosen Mg II algorithm and the reasoning which underlie the design choices. The solar UV spectral irradiance in the region of the Mg II absorption feature is displayed at three different resolutions in the figure below. At highest resolution, we see that the Mg II feature is made up of two overlapping absorption lines each having an emission core, commonly referred to as H & K. The H & K emission cores are chromospheric emissions which vary strongly with solar activity. The pseudo-continuum irradiance – i.e. away from absorption lines – originates in the relatively weakly varying upper photosphere. The Mg II index owes its great value to close proximity in wavelength of the strongly and weakly varying wavelength regions. Changes in instrumental responsivity typically vary slowly with wavelength. In order to derive an accurate gauge of solar activity, we exploit these properties in the Mg II index definition. It is defined as the ratio of the core irradiance to that of the nearby wings. Both the numerator and denominator are proportional to the instrumental responsivity, and so this unwanted dependence is cancelled in the ratio. The Mg II index has been derived from the measurements from several experiments. Although each is a core to wing ratio, the precise definitions are always different, adapting to the strengths and weaknesses of each individual instrument and data set.
The underlying SUSIM UV measurements were gathered at 1.1 nm resolution sampled approximately every 0.24 nm. The figure below shows the measurements on instrumental wavelengths for one day's scan.

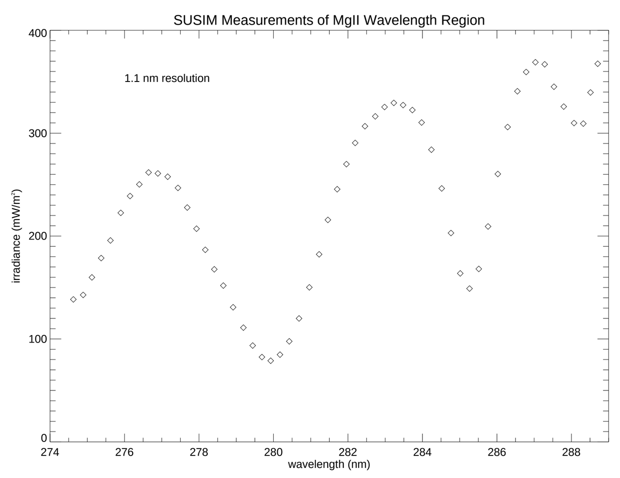

As one can see in the figure, only the broadest structures remain. For the numerator, we integrate over the core portion centered on the nadir point as determined by parabolic fit. The denominator was generally chosen to be a linear combination of separate integrations of the three nearest peaks. A constraint that was applied to the determination of these constants was that the resulting index should be insensitive to responsivity changes which are linear with respect to wavelength. Consistent with this constraint, the particular choices for integration regions and the weights were determined through an optimization process in which the ratio of high frequency noise to the strength of the solar rotation periodicity was minimized. This ratio was established using the DFT/CLEAN spectral decomposition of the Mg II time series for each parameter choice (Crane, 2001).
Quantitatively, the SUSIM Mg II index, M, is defined to be

$$M = \frac{i_2}{c_1 i_1 + c_3 i_3} \tag{1}$$

where i_n is the average irradiance found at the two peaks, labeled 1 and 3, and the core, labeled 2. The constants c_1 and c_3 are determined by the constraints:

$$c_1 = \frac{\lambda_3 - \lambda_2}{\lambda_3 - \lambda_1} \qquad c_3 = \frac{\lambda_2 - \lambda_1}{\lambda_3 - \lambda_1} \tag{2}$$

The optimization process yielded the following values for the integration regions

$$\Delta\lambda_1 = .400nm \qquad \Delta\lambda_2 = .550nm \qquad \Delta\lambda_3 = .535nm \tag{3}$$

Relationship of Mg II Index to Measurements of Irradiance

The linear relationship between the Mg II index and UV spectral irradiance measurements is well established (Heath & Schlesinger, 1986; Cebula & DeLand, 1992; Floyd et al., 2004). This has led to its use as a proxy for the UV irradiance (Tobiska et al., 2000). Although there exist differences between the Mg II times series and that of spectral irradiances at other wavelengths, these have usually been found to be caused by short-term differences in the center-to-limb variations of active regions (Crane et al., 2004). A similar relationship has been shown for EUV measurements of the He II 30.4 nm line which emerges in the lower part of the transition region (Viereck et al., 2001). More recently, time series of coronal lines derived from EIT images (e.g. Fe XV) have been shown to correlate better with Mg II than with $F_{10.7}$ (Floyd et al., 2004).

Here we consider the separate correspondence between the short- and long-term components of Mg II and solar irradiance time series. Fröhlich (2004) finds that the contribution of bright regions (i.e. faculae and network) to the total solar irradiance (TSI) can be better modeled by a three component model where the short- and long-term components of Mg II have separate coefficients rather than by a single Mg II term. Floyd et al. (1997) and Woods & Rottman (2001) had also found that such a three component model better described the the Ly-α irradiance from SUSIM and SOLSTICE, respectively, than did a linear model. Since that time, the Ly-α irradiance measurements have been updated for both experiments. The figure below displays the SUSIM Ly-α irradiance time series, a linear fit with Mg II, and a three parameter fit with the short- and long-term components separated. Below the corresponding residuals are plotted.

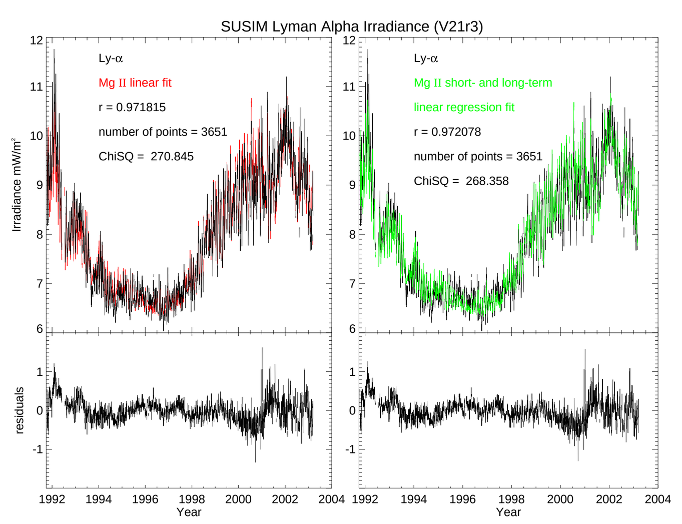

The two parameter, linear case fit the following equation:

$$L = a + bM \tag{4}$$

where $L$is the Ly-α irradiance and M is the Mg II index In the three parameter case, the following equation is fit:

$$L = a + b\bar{M} + c(M - \bar{M}) \tag{5}$$

The long-term component $\bar{M}$ was calculated by convolving the Mg II index with a 81-day FWHM Gaussian function. The short-term component is the difference between Mg II and its long-term component, i.e. $M - \bar{M}$.

The results show that while the extra term in the fit is statistically significant, the residuals show little improvement. Thus observing the high correlation, we may conclude that the SUSIM Ly-α irradiance is effectively explained by a model that is linearly related to the Mg II index. This contrasts with the aforementioned earlier results.

A similar procedure is followed for the SEM He II 30.4 nm irradiance. The plot is displayed below.

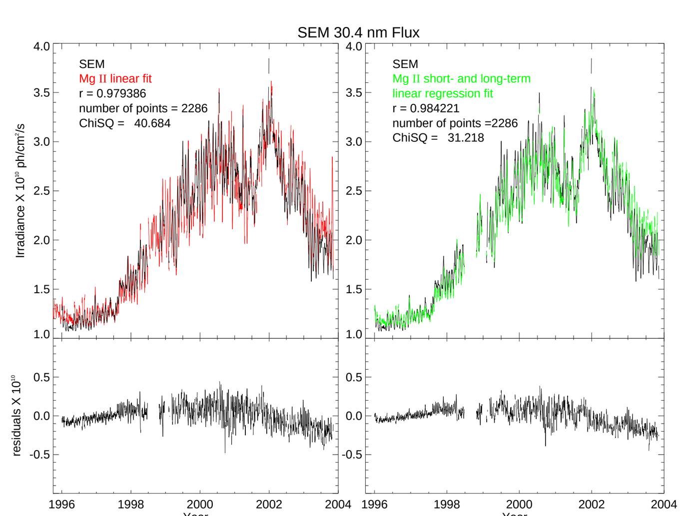

By contrast to the Ly-α result, the residuals in the He II case show significant improvement in the 3 parameter fit. We expect that this improvement is made possible by differences in the center-to-limb behavior of He II and Mg II.

The inconsistent results for TSI, Ly-α, and He II indicate that a greater understanding of the underlying physical mechanisms is needed.

Comparisons with Mg II Indices from Other Experiments

Below are displayed Mg II indices gathered during the last decade from three instruments, SOLSTICE, SUSIM, and GOME having underlying instrumental resolutions of 0.20 nm, 1.1 nm, and 0.17 nm, respectively (deToma et al., 1999; Floyd et al., 1998; Weber et al., 1998).

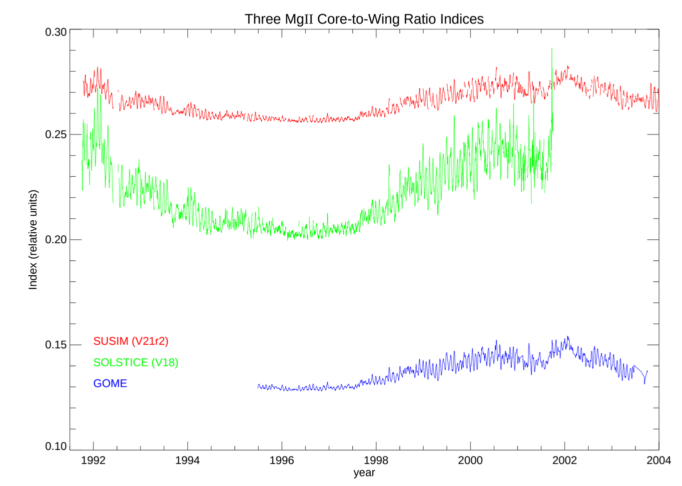

The plots below show these same indices when linearly least squares fitted to one another; the high correlations (>0.98) demonstrate their high quality linear dependence despite differences in how the indices are precisely defined.

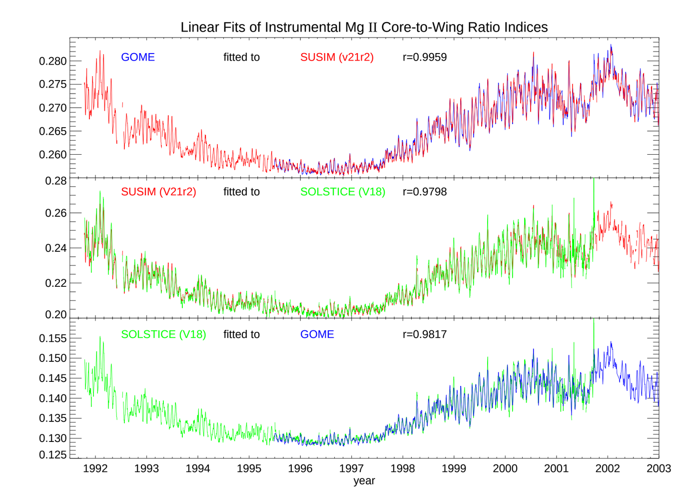

Time Series Spectral Analysis Comparisons with GOME

The SUSIM V21r2 Mg II index time series is further compared with that of GOME in the frequency transform domain. Only the data from each experiment that were available for days in common were analyzed. These two reduced times series, each containing 2134 data points spanning a time period from 27 June 1995 to 1 October 2003 were transformed into the frequency domain using the DFT/CLEAN algorithm as described by Crane (2001). In addition the entire SUSIM V21r2 Mg II time series was also so transformed. The results for SUSIM and GOME for days in common, as well as for the entire SUSIM time period are displayed in the four figures below.

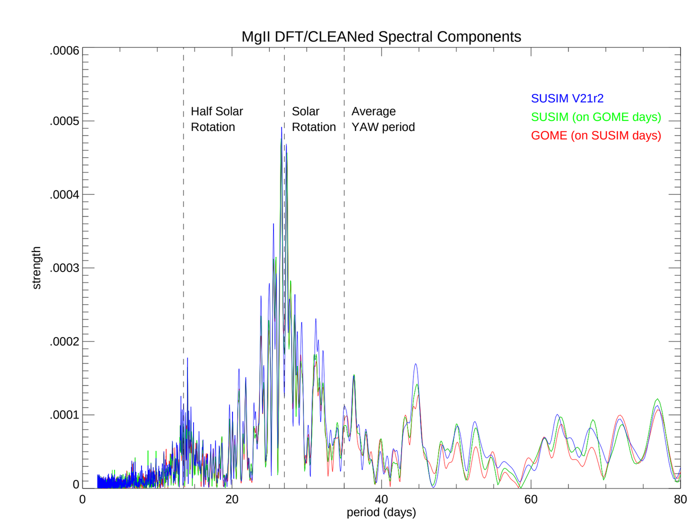

The shortest periods are displayed in the first plot. Generally, the GOME and the two SUSIM periodic behaviors are quite similar. The solar rotation and half solar rotation are displayed. These periodicities do not manifest themselves as a single peak, but rather a group of closely spaced peaks. The reason for this is that the periodicity is not stationary because the phase of the two periodicities changes from time to time as active regions decay and new ones are formed. The average UARS yaw-around period is about 35 days and it appears that the only periodicity nearby is also experienced by GOME (which, unlike SUSIM, is not aboard the UARS). Thus, we may conclude that there is no detectable corruption of the SUSIM Mg II time series by UARS yaw-arounds.

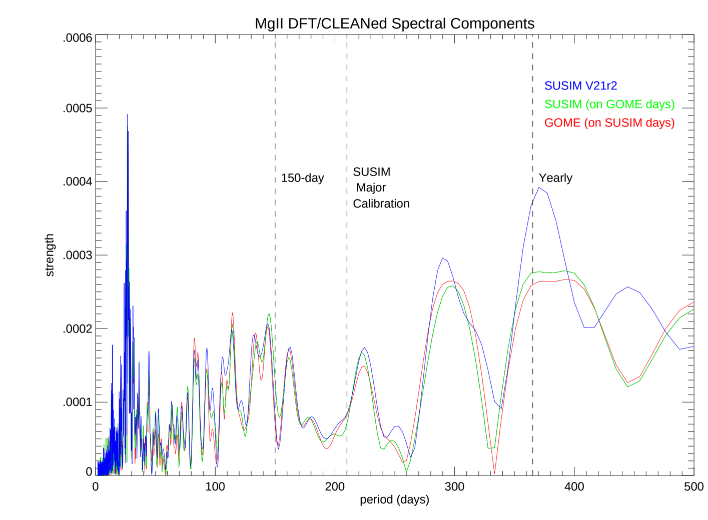

The next plot continues to show good agreement among the three cases. Well known solar periodicities of 150 and 300 days are present in all three. Although there is a peak near the period corresponding to SUSIM major calibrations (210 days), this is also shared by GOME for which this periodicity has no special significance. The yearly peak of the entire SUSIM data set is clearly larger than for the other two. A likely cause of such a periodicity is the 7° offset in the solar equator from the ecliptic which is more pronounced in longer data sets.

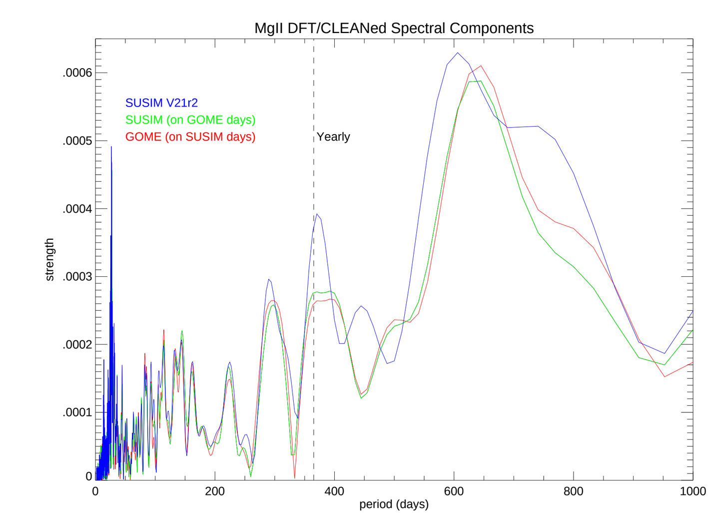

There continues to be strong agreement among the periodicities of the time series. The strong peak at 600 days has an unknown cause.

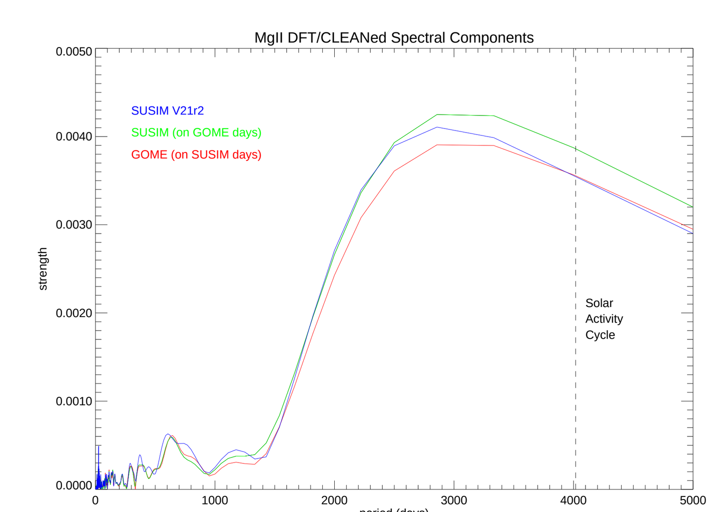

The peak corresponding to the 11 year solar activity period is common to each of the three time series. It is offset from its actual periodicity because of the relatively short duration of the Mg II index time series.

Through spectral comparisons with GOME, we find no evidence that that the SUSIM V21r2 Mg II index time series is corrupted by calibration or spacecraft influences.

Comparisons with Other Solar Activity Indices

Solar total and spectral irradiance are known to vary with solar activity. We consider four solar activity indices, the international sunspot number (ISN), the $F_{10.7}$ radio flux, the He 1083 nm Equivalent Width, and Mg II (Tapping, 1987; Donnelly et al., 1986; Viereck & Puga, 1999). Each of these is understood to be a proxy for the contribution of bright surface features to irradiance. Here we use the NOAA SEC Composite instead of the SUSIM Mg II because the former spans a greater period of time. The $F_{10.7}$ index is the 10.7 cm radio flux measured the ground daily since 1947. The He 1083 nm Equivalent Width (He 1083) is the width of the solar 1083 nm infared absorption line assembled from ground based solar images obtained since 1974. These time series are displayed below. Also plotted is long-term (filtered) version of each time series which was produced by convolving the original time series with the 81-day FWHM Gaussian function. This convolution effectively removes (i.e. smooths over) the effects which occur on solar rotation time scales.

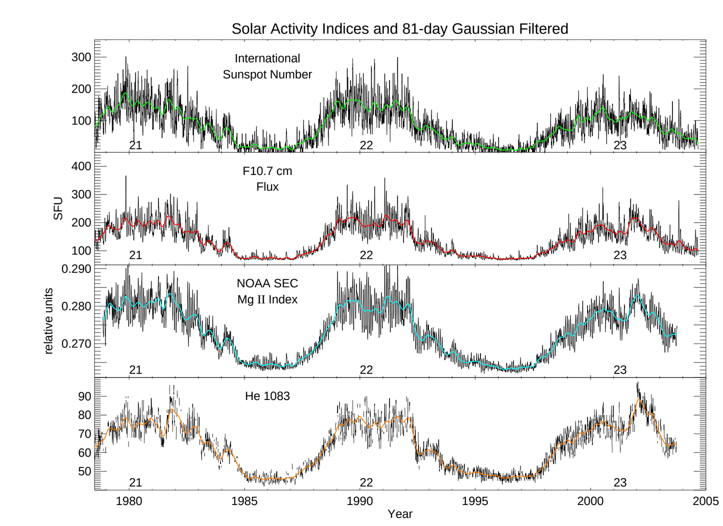

We compare these smoothed time series by finding the linear relationship with each of the others while including only those data common to all. This allows comparision of the quality of the data themselves while removing the dependence on the number of data points. Plotted below is the case where Mg II is fitted by the other three. Below the figure are two tables showing the correlations of the long and short-term components of each index to the others. (The short-term component is equal to the difference between the index and its 81-day filtered version.)

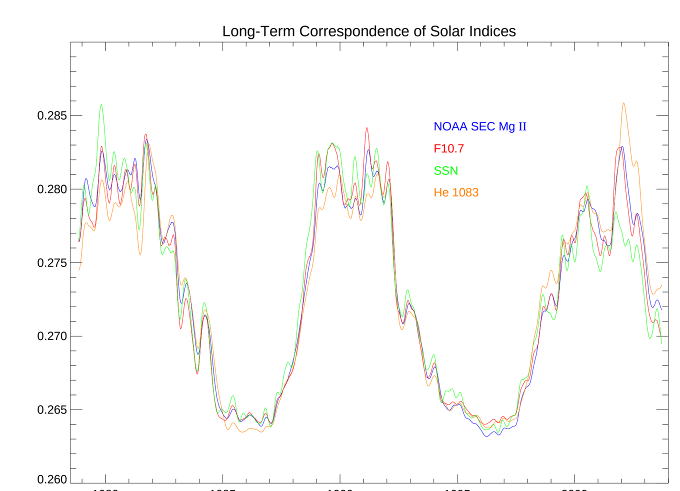

Long-Term	ISN	$F_{10.7}$	Mg II	He 1083
ISN	1.000	0.981	0.974	0.935
$F_{10.7}$	0.981	1.000	0.992	0.966
Mg II	0.974	0.992	1.000	0.980
He 1083	0.935	0.966	0.980	1.000

Short-Term	ISN	$F_{10.7}$	Mg II	He 1083
ISN	1.000	0.804	0.700	0.631
$F_{10.7}$	0.804	1.000	0.769	0.675
Mg II	0.700	0.769	1.000	0.855
He 1083	0.631	0.675	0.855	1.000

Through these comparisons of ISN, $F_{10.7}$, He, and Mg II, we observe:

- their long-term behavior is quite similar, especially Mg II and $F_{10.7}$,
- during the secondary peak of the Solar Cycle 23 maximum:
  - ISN did not experience the 2nd peak near the end of 2001
  - He 1083 was significantly higher than the others
- no secular trend in level of the minima are observed.

Summary and Conclusions

In this study, we describe and analyze the correspondence of the SUSIM Mg II index time series to irradiances and other solar indices. In concluding, we find that:

- the need for separate long- and short-term components of Mg II to describe solar irradiances is an open question,
- the correspondence with Mg II indices from other experiments is very close,
- no evidence that the SUSIM Mg II index time series is corrupted by instrumental calibration or spacecraft influences, implying …
- … that the measurements reflect actual solar behavior, and
- the Mg II index and $F_{10.7}$ share a similar long-term behavior as compared with other solar indices (ISN and He I 1083 cm).

Acknowledgements

We thank the many institutions and individuals who provided data used in this study. Rodney Viereck of NOAA SEC provided the most recent Mg II composite index. The He 1083 data are derived from NSO/Kitt Peak data which are produced cooperatively by NSF/NOAO, NASA/GSFC, and NOAA/SEL. Data for SOLSTICE (PI: Gary Rottman) and for for SEM (PI: Darrell Judge) were retrieved from their WWW sites. The International sunspot number and $F_{10.7}$ flux were obtained from the National Geophysical Data Center. SOHO is a mission of international cooperation between ESA and NASA.

Bibliography

Brueckner, G. E., Edlow, K. L., Floyd, L. E., Lean, J. L., and Vanhoosier, M. E. (1993). The solar ultraviolet spectral irradiance monitor (SUSIM) experiment on board the Upper Atmosphere Research Satellite (UARS). *J. Geophys. Res.*, 98:10695–+.

Cebula, R. P., Deland, M. T., and Schlesinger, B. M. (1992). Estimates of solar variability using the solar backscatter ultraviolet (SBUV) 2 Mg II index from the NOAA 9 satellite. *J. Geophys. Res.*, 97:11613–11620.

Crane, P., Floyd, L., Cook, J., Herring, L., Avrett, E., and Prinz, D. (2004). The Center-to-Limb Behavior of Solar Active Regions at Ultraviolet Wavelengths. *A&A*, 419:735–746.

Crane, P. C. (2001). Applications of the DFT/CLEAN Technique to Solar Time Series. *Sol. Phys.*, 203:381–408.

de Toma, G., White, O. R., Knapp, B. G., Rottman, G. J., and Woods, T. N. (1997). Mg II core-to-wing index: Comparison of SBUV2 and SOLSTICE time series. *J. Geophys. Res.*, 102:2597–2610.

Donnelly, R. F., Hinteregger, H. E., and Heath, D. F. (1986). Temporal variations of solar EUV, UV, and 10,830-A radiations. *J. Geophys. Res.*, 91:5567–5578.

Floyd, L., Brueckner, G., Crane, P., Prinz, D., and Herring, L. (1997). Correlations of Solar Cycle 22 UV Irradiance. In *ESA SP-415: Correlated Phenomena at the Sun, in the Heliosphere and in Geospace*, pages 235–+.

Floyd, L., Newmark, J., Cook, J., Herring, L., and McMullin, D. (2004). Solar EUV and UV Spectral Irradiances and Solar Indices. *Journal of Atmospheric and Solar-Terrestrial Physics*, page in press.

Floyd, L. E., Reiser, P. A., Crane, P. C., Herring, L. C., Prinz, D. K., and Brueckner, G. E. (1998). Solar Cycle 22 UV Spectral Irradiance Variability: Current Measurements by SUSIM UARS. *Sol. Phys.*, 177:79–87.

Fröhlich, C. (2004). Solar Irradiance Variability. In Pap, J. M., Fox, P., Fröhlich, C., Hudson, H. S., Kuhn, J., McCormack, J., North, G., Sprigg, W., and Wu, S., editors, *Solar Variability and its Effect on the Earth's Atmosphere and Climate System*, pages 97–110. American Geophysical Union, Washington, DC.

Heath, D. F. and Schlesinger, B. M. (1986). The Mg 280-nm doublet as a monitor of changes in solar ultraviolet irradiance. *J. Geophys. Res.*, 91:8672–8682.

Tapping, K. F. (1987). Recent solar radio astronomy at centimeter wavelengths - The temporal variability of the 10.7-cm flux. *J. Geophys. Res.*, 92:829–838.

Tobiska, W. K., Woods, T., Eparvier, F., Viereck, R., Floyd, L., Bouwer, D., Rottman, G., White, O. R., and Donnelly, R. F. (2000). The SOLAR2000 Empirical solar irradiance model and forecast tool. *Journal of Atmospheric and Solar-Terrestrial Physics*, 62:1233–1250.

Viereck, R., Puga, L., McMullin, D., Judge, D., Weber, M., and Tobiska, W. K. (2001). The Mg II Index: A Proxy for Solar EUV. *Geophys. Res. Lett.*, 28:1343–1346.

Viereck, R. A. and Puga, L. C. (1999). The NOAA Mg II core-to-wing solar index: Construction of a 20-year time series of chromospheric variability from multiple satellites. *J. Geophys. Res.*, 104:9995–10006.

Weber, M., Burrows, J. P., and Cebula, R. P. (1998). Gome Solar UV/VIS Irradiance Measurements between 1995 and 1997 - First Results on Proxy Solar Activity Studies. *Sol. Phys.*, 177:63–77.

Woods, T. N., Rottman, G. J., and Ucker, G. J. (1993). Solar-Stellar Irradiance Comparison Experiment 1. II - Instrument calibrations. *J. Geophys. Res.*, 98:10679–+.

Woods, T. N., Tobiska, W. K., Rottman, G. J., and Worden, J. R. (2000). Improved solar Lyman α irradiance modeling from 1947 through 1999 based on UARS observations. *J. Geophys. Res.*, 105:27195–27216.